Since January 2020 Elsevier has created a COVID-19 resource centre with free information in English and Mandarin on the novel coronavirus COVID-19. The COVID-19 resource centre is hosted on Elsevier Connect, the company's public news and information website.

Chemical Engineering Science 230 (2021) 116206

Contents lists available at ScienceDirect

Chemical Engineering Science

journal homepage: www.elsevier.com/locate/ces

Use of semibatch reactor technology for the investigation of reaction mechanism and kinetics: Heterogeneously catalyzed epoxidation of fatty acid esters

Wander Y. Perez-Sena [a,b], Johan Wärnå [a], Kari Eränen [a], Pasi Tolvanen [a], Lionel Estel [b], Sébastien Leveneur [a,b], Tapio Salmi [a,*]

[a] Laboratory of Industrial Chemistry and Reaction Engineering, Johan Gadolin Process Chemistry Centre, Åbo Akademi University, FI-20500 Åbo-Turku, Finland
[b] Normandie Université, INSA Rouen, UNIROUEN, LSPC, EA4704, FR-76000 Rouen, France

HIGHLIGHTS

- Greener and safer production of epoxidized vegetable oil.
- Positive effect of semibatch operation on the reaction performance.
- Kinetic modelling based on plausible mechanism for the alumina catalyzed epoxidation.

ARTICLE INFO

Article history:
Received 21 July 2020
Received in revised form 8 October 2020
Accepted 10 October 2020
Available online 14 October 2020

Keywords:
Semibatch operation
Kinetics
Reaction mechanism
Vegetable oils epoxidation
Heterogeneous catalyst

ABSTRACT

Heterogeneously catalyzed epoxidation of vegetable oils by hydrogen peroxide represents a greener route for the production of epoxides and a thermally safer reaction route compared to the classical Prileschajew epoxidation approach. The epoxidation kinetics of the heterogeneous system formed by aluminium oxide catalyst, hydrogen peroxide and methyl oleate as a model compound was studied with semibatch experiments in laboratory scale. It was found that semibatch operation improved the performance significantly compared to classical batch operation, a low and constant volumetric flowrate of hydrogen peroxide increased the final oxirane yield considerably. A semibatch reactor model and a kinetic model were developed, featuring the reaction temperature, the reactant molar ratio, the catalyst loading and the mass flow rate as the most significant experimental parameters. The mathematical model was able to well describe the experimental data. The approach can be applied to other liquid–solid catalyst systems in future in order to optimize the semibatch operation policy for complex reaction systems.

1. Introduction

In the past decades, academic and industrial researchers have turned their interest to the exploration of new sources of chemicals and energy instead of fossil fuel resources (Cherubini, 2010; Tuck et al., 2012; Sheldon, 2014). The main motivation is an eventual depletion of oil resources and the need to diminish the pollution associated to their utilization. Therefore, the research is nowadays keenly looking for alternative sources of raw materials with a more environmentally friendly approach. Biomass valorization is one of the most promising fields of investigation in this matter. An important amount of methods and procedures for the application of biomass as an ecofriendly source of chemicals and fuels have been developed (Sheldon, 2014; Mohanty et al., 2002). Among the valuable components of biomass, vegetable oils represent very advantageous feedstock.

Vegetable oils are an abundant source of raw materials for the production of fuels, fine chemicals, polymers, and chemical intermediates. (Mohanty et al., 2002; Biermann et al., 2011; Richard et al., 2013; Murawski et al., 2018). Hence the arising interest in their utilization and their derivatives as renewable feedstock for the production of added-value products. One of the most promising routes of valorization is the transformation of the double bonds in vegetable oils to epoxides (Freites Aguilera et al., 2018; Danov et al., 2017). The main method for the production of epoxidized vegetable oils is the Prileschajew epoxidation (current industrial process) (Freites Aguilera et al., 2019), which consists of a biphasic system with an oxidant agent (mainly hydrogen peroxide), an oxygen carrier (percarboxylic acid) and the unsaturated vegetable oil.

* Corresponding author.

https://doi.org/10.1016/j.ces.2020.116206
0009-2509/

Nomenclature

a	merged parameter in rate equation
c	concentration
c_0	total concentration of adsorption sites on catalyst surface
k	reaction rate constant
m	mass
n	amount of substance
r	catalytic reaction rates
r'	non-catalytic reaction rates
t	time
V	volume
V'	volumetric flow rate
$\alpha, \beta, \gamma, \omega$	merged rate parameters
λ	empirical exponent in rate equation
ν	stoichiometric number
ρ	density
τ_0	ratio between initial volume-to-volumetric flow rate

Subscripts and superscripts

B	bulk
i, j	component index
L	liquid
0	inlet or initial quantity
*	surface site

Abbreviations

DB	component with a double bond, e.g. fatty acid ester
HP	hydrogen peroxide
OH	hydroxyl group
OOH	hydroxylperoxide adduct
O	Oxygen
EP	epoxidized product
W	Water
*	vacant site on the catalyst surface
EXP	experimental
SIM	simulation
OF	objective function
R^2	coefficient of determination

Abbreviations OH*, I* etc. denote the corresponding adsorbed species on the catalyst surface.

Homogenous and heterogeneous catalysts (mainly mineral acids and solid resin catalysts with sulphonic acid groups) have been applied to enhance the formation of percarboxylic acid (Vianello et al., 2018; Zheng et al., 2015). The percarboxylic acid is produced in situ through perhydrolysis of a carboxylic acid with hydrogen peroxide. The percarboxylic acid then diffuses to the organic phase to react with the double bonds and form an epoxide. At an industrial scale some key market players using Prileschajew system for production of epoxidized vegetable oils are Arkema SA (France), CHS INC (U.S.), Ferro corporation (U.S.), Hairma chemicals (GZ) Ltd (China) (ESBO, 2020). Epoxidized vegetable oils find applications as additives or plasticizers in paint, coating or PVC (Horvath and Malacria, 2020).

Some other methods for the production of epoxides have also been reported in the literature (Santacesaria et al., 2011; Mandelli, 2001; Scotti et al., 2015; Sepulveda et al., 2007; Gunam Resul et al., 2018; Li et al., 2006; Phimsen et al., 2017; Parada Hernandez et al., 2017; Turco et al., 2017; Nur et al., 2001; Campanella et al., 2004; Goud et al., 2007), such is the case of the direct epoxidation with an oxidant agent (i.e. hydrogen peroxide, TBHP, O_2) in the presence of a heterogeneous catalyst. These heterogeneous methods present a greener approach. By avoiding the use of carboxylic acid, no perhydrolysis takes place in the system, which contributes to high exothermicity, waste and troublesome separation of the final products. In addition, the impact of undesired reactions, such as ring opening is diminished by applying direct epoxidation with an oxidant agent like hydrogen peroxide as only reagent. Recently, a thermal risk assessment has been carried out by our group (Pérez-Sena et al., 2020), in which the classical Prileschajew method was compared to the alumina catalyzed epoxidation, and the latter one was found to present less risk with a lower probability of thermal runaway.

Some works have shown the catalytic capability of alumina to epoxidize various vegetable oils such as oleic acid, soybean oil, castor oil (Sepulveda et al., 2007; Parada Hernandez et al., 2017; Turco et al., 2016; Miao and Liu, 2014; Suarez et al., 2009) and their methyl esters. However, only few kinetic models have been developed for this system mostly featuring small substrates (i.e. alkenes epoxidation reactions) (Zapata et al., 2010; Bonon et al., 2014). According to our knowledge, no kinetic model has been proposed so far in the open literature for the epoxidation of vegetable oils using alumina as a heterogeneous catalyst.

In order to improve the efficiency of this promising heterogeneous catalytic system, it is essential to obtain a better understanding of the reaction mechanism and kinetics. Moreover, this reaction has mainly been studied in batch mode. It is therefore of crucial interest to explore alternative reactor technologies and to investigate how the reactor technology, particularly the mode of operation would influence the final product distribution because many parallel and consecutive reactions take place in the system, for instance hydrogen peroxide decomposition and ring opening of the epoxide.

Two different operation modes were compared for the heterogeneously catalyzed epoxidation of methyl oleate in the presence of an aluminium oxide catalyst: batch and semibatch operation. A semibatch operation mode was found to have a beneficial effect on the epoxidation reaction by introduction of the hydrogen peroxide over the reaction time. Thereafter, a kinetic model was developed based on plausible reaction mechanisms and taking into consideration both the catalytic and non-catalytic reactions of the system. Numerical regression analysis was performed and the kinetic parameters were estimated. The statistical analysis of the kinetic parameters demonstrated their good reliability. The developed model can successfully simulate the course of the reaction and its respond to experimental parameters. Reaction temperature, catalyst loading, reactant molar ratio and flow rate are the main parameters of semibatch operation.

2. Experimental section

2.1. Materials

The following chemicals were used: oleic acid (purity $\geq$ 90%), methanol (purity $\geq$ 99%), sulfuric acid (purity $\geq$ 99%), hydrogen peroxide (purity $\geq$ 33 wt%), magnesium oxide, tetrabutyl ammonium bromide, acetic acid, Hanus solution 0.1 N were all purchased from Sigma Aldrich and used as received. γ-Alumina (Versal GH) was provided by LaRoche Chemicals.

2.2. Catalyst characteristics

Versal GH (LaRoche Chemicals) was utilized as the epoxidation catalyst, which is a high-performance catalytic grade aluminium oxide. This γ-alumina has been used by our group in a previous investigation (Eränen, 2004). Therefore, the catalyst characteristics are summarized from the previous research and as well as from data provided by the manufacturer in Table 1.

2.3. Analytical methods

All the samples withdrawn from the reactor were centrifuged. The aqueous and organic phases were separated and analyzed independently right after the experiment was finished.

The oxirane content (i.e., epoxide groups), in the samples, was quantified by Jay's method (Jay, 1964; Paquot, 2013; Swern et al., 1947) in which samples are dissolved in chloroform, followed by addition of a 20 wt% solution of tetraethylammonium bromide (TEAB) and finally titrated with a standard 0.1 M perchloric acid solution. An automatic titrator (799 GPT Titrino, Metrohm) was used.

The double bond concentration was determined through titration of the iodine value by using traditional Hanus' method (Paquot, 2013; I. TC 34/SC 11, 1996).The hydrogen peroxide concentration determined by the ceric sulfate titration method (Greenspan and MacKellar, 1948). The details of the procedure and samples pretreatment are provided in supplementary material.

2.4. Esterification of oleic acid

Methyl oleate was prepared in a 500 mL glass reactor equipped with a mechanical stirrer and a reflux condenser. Vigorous stirring was applied (800 rpm) to suppress the external mass transfer limitation. Oleic acid (OA), methanol and sulfuric acid were mixed in a 19.2%, 79.8, 1% molar percentage as indicated by Nicolau et al. (2010). After three hours, the reaction was let to stratify and the organic phase was washed with distilled water five times. The organic phase was then purified by removing water and traces of methanol in a vacuum rotatory evaporator (LABOROTA 4000, Heidolph) and later dried over a molecular sieve. A 90% conversion of the oleic acid to methyl ester was confirm by acidity titration method (Wu et al., 2016).

2.5. Epoxidation of methyl oleate in the presence of γ-alumina

A mixture of methyl oleate, the catalyst and ethyl acetate as solvent was poured into a 500 mL glass reactor equipped with mechanical agitation (800 rpm), baffles and a reflux condenser (Fig. 1). As the reaction mixture reached the desired temperature, hydrogen peroxide was added dropwise into the reactor vessel with a peristaltic pump. The reaction was continued under isothermal conditions for 24 h with periodical sampling.

A wide set of conditions was screened to reveal the qualitative behavior of the system and to collect enough data for the parameter estimation stage. Table 2 provides an overview of the conducted kinetic experiments. The double bond-to-hydrogen

Table 1
Principal characteristics of the catalyst.

	Chemical Analysis (wt%)							Physical Properties			
	Na_2O	Fe_2O_3	SiO_2	SO_4	Cl	Al_2O_3 by difference	LOI*	Loose Bulk density ($g{\cdot}mL^{-1}$)	Surface Area ($m^2{\cdot}g^{-1}$)	Acid Dispersibility (%)	Phase
Versal GH	0.07	0.04	0.1	0.03	0.1	96.7–98.7	1–3	0.59	270	<10	Gamma

*Loss on ignition.

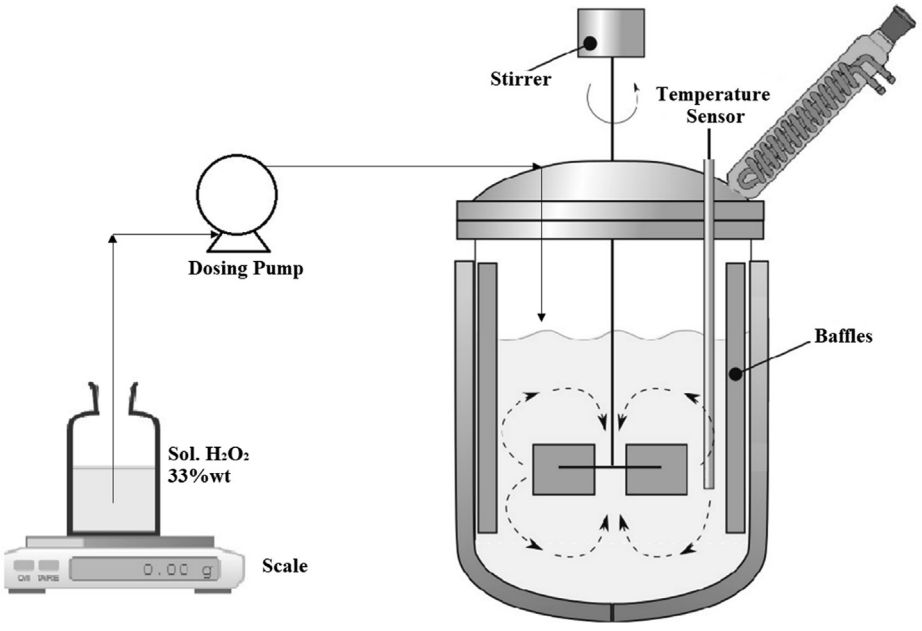

Fig. 1. Simplified scheme of the reactor system.

Table 2
Experimental matrix for epoxidation system.

Experiment	DB: HP	wt% Catalyst	Temperature (°C)	Q ($g \cdot min^{-1}$)	Addition time (min)
Run1	1:5.8	10	50	0.23	502
Run2	1:5.8	10	60	0.22	510
Run3	1:5.7	10	70	0.22	510
Run4	1:5.8	10	74	0.23	496
Run5	1:5.7	10	76	0.59	191
Run6	1:5.7	10	76	1.15	98
Run7	1:5.8	10	76	4.32	27
Run8	1:5.8	0	74	0.22	513
Run9	1:5.8	2	74	0.21	540
Run10	1:5.8	5	76	0.23	488
Run11	1:4	13	74	0.22	332
Run12	1:7.2	10	74	0.23	622
Run13	1:4	10	74	1.08	71
Run14	1:4	10	74	4.53	17
Run15	1:4	10	74	Batch	–
Run16	0:1	0	60	Batch	–
Run17	0:1	0	70	Batch	–
Run18	0:1	0	80	Batch	–
Run19	1:4	0	70	Batch	–
Run20	1:4	0	80	Batch	–

Solvent: ethyl acetate Q = mass flow of hydrogen peroxide solution.

peroxide molar ratio, the catalyst loading, the reaction temperature and the mass flow were the experimental parameters

Besides the catalytic epoxidation experiments, two different sets of non-catalytic experiments were also carried out to investigate their contribution to the overall rate: non-catalytic hydrogen peroxide decomposition and non-catalytic epoxidation. During the hydrogen peroxide decomposition experiments, a fixed amount of 33 wt% hydrogen peroxide solution was set to decompose in the 500 mL glass reactor in batch operation. The reaction temperature was the experimental parameter. Similarly, in the non-catalytic epoxidation experiments, a mixture of methyl oleate and 33 wt% hydrogen peroxide solution was loaded into the 500 mL glass reactor and the batch experiment was started.

3. Experimental results and discussion

3.1. Epoxidation reaction

3.1.1. Influence of experimental parameters

As previously mentioned, the aims of this work are to investigate the effect of the reactor configuration on the alumina-catalyzed epoxidation and to develop a kinetic model based on a plausible reaction mechanism. Therefore, it is possible to summarize the influences of some operational parameters such as optimal catalyst loading, reaction temperature and reactant molar ratio on the epoxidation rate. These effects have already been studied by various groups of researchers (Mandelli, 2001; Sepulveda et al., 2007; Parada Hernandez et al., 2017; Turco et al., 2016; Miao and Liu, 2014.

It was re-confirmed that an increase of the catalyst loading increases the yield of oxirane proportionally (Fig S1 in Supplementary material), but, an increase exceeding 10 wt% does not seem to improve significantly the final yield of the product. As the catalyst amount exceeded 10 wt%, the proportionality between the reaction rate and the active element concentration was not maintained, which could be due to rapid side catalytic hydrogen peroxide decomposition when high amount of catalyst are loaded. The influence of temperature was also investigated (Fig S2) and as expected, the epoxidation kinetics was enhanced with an increasing temperature resulting in a higher reactant conversion and product yield. However, the maximum operating temperature that can be reached in the system is limited by the boiling point of the solvent, in this case ethyl acetate (77 °C under atmospheric pressure). From Fig S3 the optimal double bond-to-hydrogen peroxide molar ratio was confirmed to be at around 1:6 as corroborated by Sepulveda et al. (Sepulveda et al., 2007) in their research. A further increase of this ratio did not result in any significant improvement of the final yield and conversion. The highest double bond conversion and epoxy yield observed were 90% and 82% respectively when maximum temperature, lowest hydrogen peroxide mass flow, 1:6 reactant molar ratio and 10 wt% catalyst were applied.

3.1.2. Influence of semibatch operation

Unlike well-studied heterogeneously catalyzed epoxidation of vegetable oils in batch mode (Sepulveda et al., 2007; Parada Hernandez et al., 2017; Turco et al., 2016; Miao and Liu, 2014; Suarez et al., 2009); no literature is available for the case in which hydrogen peroxide is added gradually to the reaction system, while the rest of the reactants are loaded into the reactor. This semibatch operation mode is currently used in industrial scale in the Prileschajew epoxidation. By dosing one or more of the reactants to the reaction system, the heat evolution of this very exothermic reaction is kept controlled. Hence, secondary reactions such as the decomposition of hydrogen peroxide percarboxylic acids are diminished and a good yield of the final product is obtained.

In principle in a semibatch setup where hydrogen peroxide is continuously added over a period, its consumption depends on the dosing rate. The lower the feed rate of the reactant, the less accumulation, therefore in theory one could be even able to adjust the dosing rate to the reaction rate of hydrogen peroxide and virtually no accumulation would take place.

Fig. 2 demonstrates clearly that operation under semibatch conditions significantly improves the reactant conversion and the product yield in the epoxidation reaction: an improvement of more than 30% was observed when low-flow semibatch conditions were applied compared to batch operation under identical conditions.

It has been proposed by some researchers (Mandelli, 2001; Parada Hernandez et al., 2017; Pérez-Sena et al., 2020; Turco et al., 2016; Salem et al., 1993) that the peroxide sites formed on the catalyst surface due to the adsorption of hydrogen peroxide are either utilized to epoxidize the double bond or released in the form of molecular oxygen, i.e., catalyzed hydrogen peroxide decomposition. It is assumed that the overall hydrogen peroxide decomposition (non-catalyzed and catalyzed) taking place in parallel with the epoxidation of the double bond (Fig. 3) has a more rapid rate than the epoxidation process. Hence, in a batch reactor setup where a high concentration of hydrogen peroxide is present at the beginning, the decomposition rates can quickly reduce the available hydrogen peroxide, which forms active surface sites that later react with the double bond of the vegetable oil. On the other hand, when the same amount of hydrogen peroxide is loaded into the reactor gradually over an extended period, favorable conditions for the epoxidation reaction are maintained. Fig. 4 displays the hydrogen peroxide concentration evolution in both operation modes. In the batch experiment, a rapid consumption of hydrogen peroxide is evidenced: after four hours of reaction, around 50% of the total hydrogen peroxide have been consumed. This decrease of the concentration affects negatively the overall kinetics because all the reactions in the system are strongly dependent on this reagent. However, in the case of semibatch experiments, the addition of concentrated hydrogen peroxide at a constant dosing rate helped to keep an increasing concentration of hydrogen peroxide in the reactor until the addition was stopped. Thereafter, the concentration started to decrease at the same rate as in the batch experiment. From Fig. 4, it can be concluded that lower dosing rates provide a good reaction environment. By extending the total

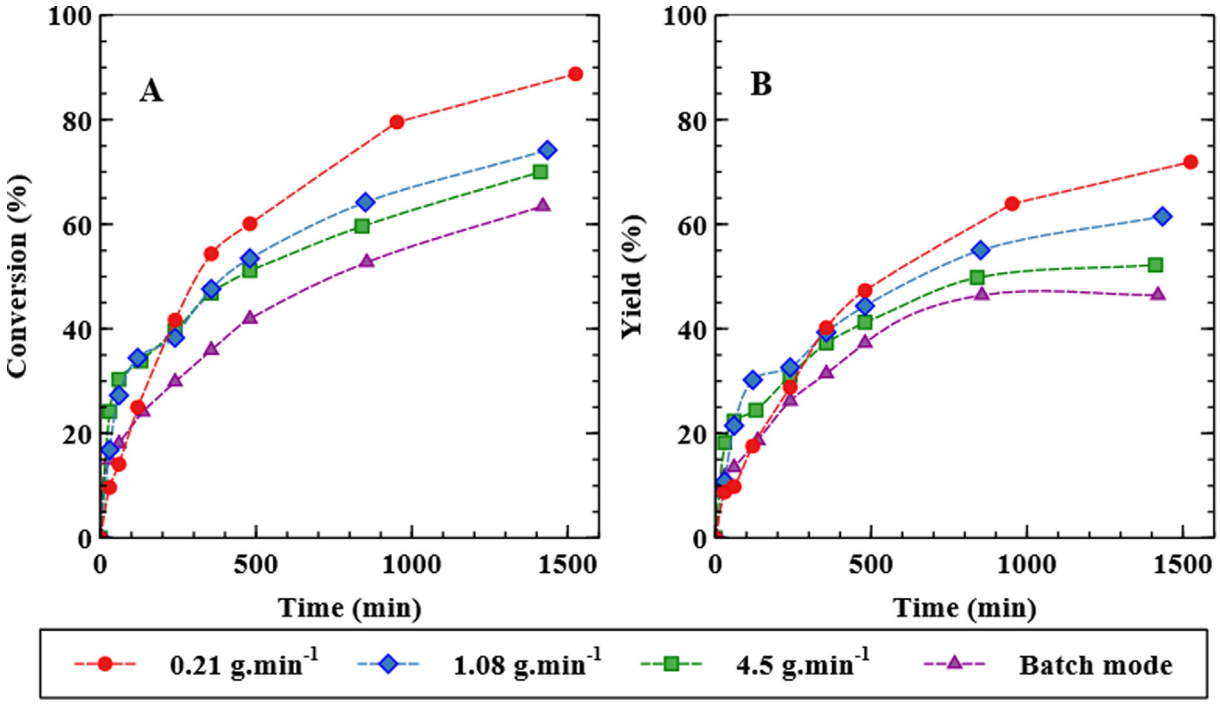

Fig. 2. Epoxidation under batch and semibatch conditions at 74 °C, DB:HP = 1:4 and 10 wt% catalyst; (a) Double bond conversion, (b) Oxirane yield.

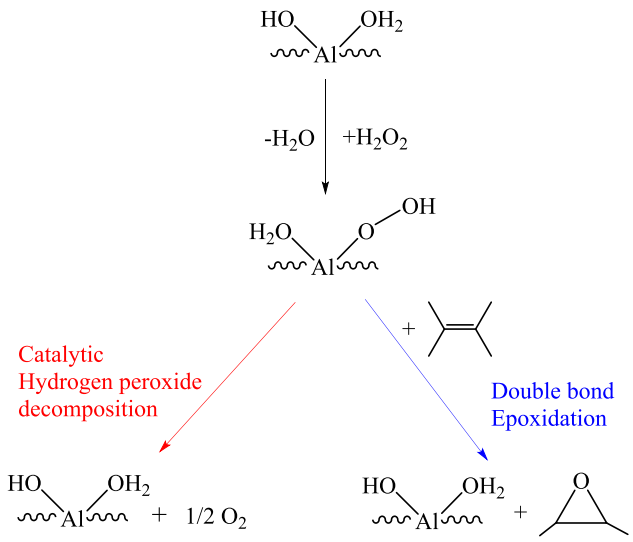

Fig. 3. Simplified reaction scheme of the catalytic epoxidation and catalytic hydrogen peroxide decomposition on the alumina surface (Mandelli, 2001; Parada Hernandez et al., 2017).

addition time and letting a fresh hydrogen peroxide solution enter the system, epoxidation kinetics is favored.

Besides that, It can also be speculated that the water always being present in the hydrogen peroxide solution is strongly adsorbed on the catalyst surface, as indicated by some studies (Mandelli, 2001; Turco et al., 2016; Lefèvre et al., 2002; Osman et al., 2017). A considerable amount of water is formed during the decomposition of hydrogen peroxide, which is highly promoted in a batch mode of operation. Water adsorption could in theory reduce the catalytic capabilities of γ-alumina by blocking the pores for the hydrogen peroxide to react and making difficult the diffusion of the olefin to the active sites (Rinaldi and Schuchardt, 2004). In this sense, the use of a more concentrated hydrogen peroxide solution (i.e. 50/70 wt%) or the use of an anhydrous hydrogen peroxide solution could probably improve the reaction outcome because of fewer water in the system as demonstrated by some researcher (Mandelli, 2001; Sepulveda et al., 2007).

3.2. Evaluation of mass transfer resistance

3.2.1. External mass transfer

The reaction limitations to operate in a kinetic regime due to external mass transport were checked following a classical but reliable test based on the quantification of the reaction productivity as the function of the stirring speed (Stamatiou and Muller, 2017; Sengupta, 2017). Because this system is a complex liquid–liquid-solid reaction, it was pertinent to determine if the interfacial mass transfer of the species had an impact on the reaction rate and the final epoxide yield.

Experiments at different stirring velocities but keeping the other parameters fixed were systematically carried out. The concentration of oxirane was utilized as the measure of productivity. Samples were analyzed at different reaction times. From Fig. 5a, it can be deduced that operation with stirring velocities exceeding 500 rpm evidently ensures enough of turbulence around the catalyst particles to remove the external mass transfer limitations. The similar product concentrations at different stirring velocities (>500 rpm) is a clear indication that the system operates in a kinetic regime.

3.2.2. Internal mass transfer

The catalyst material used in the experiments was sieved to obtain fractions with different particle diameters, after which the particle size distribution was calculated as illustrated in Fig. 6. In fact, the catalyst material mainly constituted a high percentage of fine particles (63–125 μm).

The influence of internal mass transfer, i.e., diffusion in the catalyst pores, was also checked with a classical experimental approach. The dependence of the catalytic activity on the particle size was verified by measuring the productivity, i.e. the kinetics

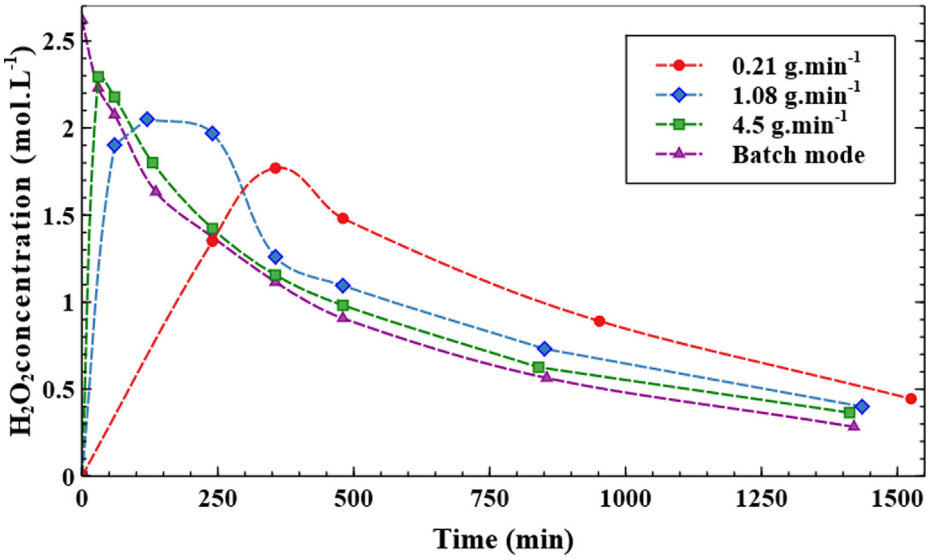

Fig. 4. Hydrogen peroxide concentration evolution under batch and semibatch conditions at 74 °C, DB: HP = 1:4 and 10 wt% catalyst.

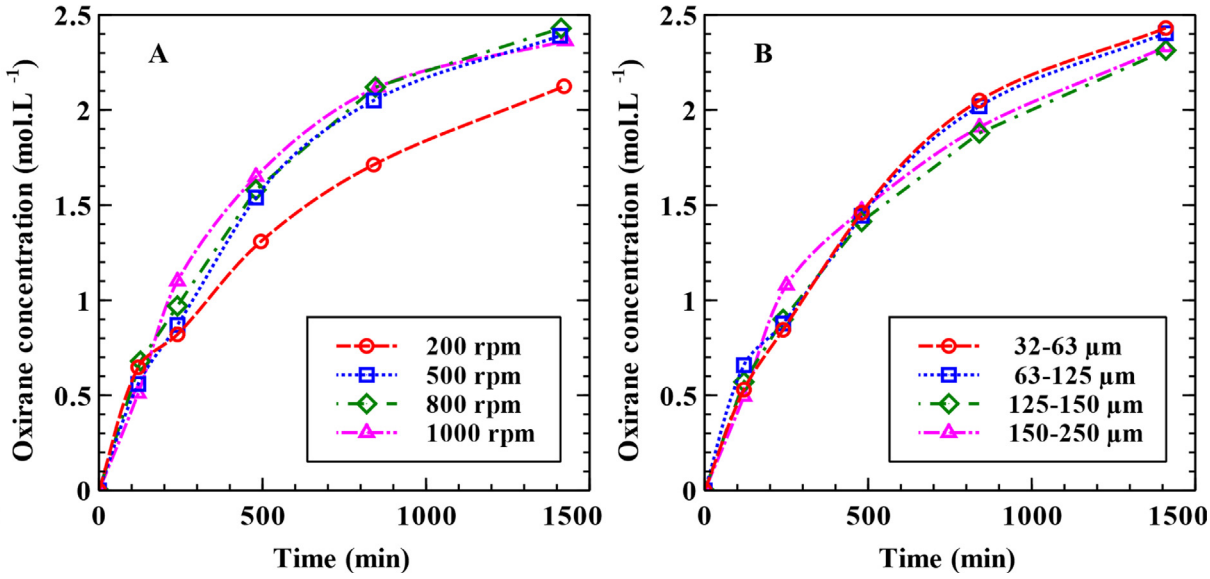

Fig. 5. Mass transfer resistance tests; (a) External mass transfer verification at 74 °C, DB:HP = 1:4, 0.22 g·min^{-1} and 10 wt%. (b) Internal mass transfer verification at 74 °C, DB: HP = 1:6, 0.22 g·min^{-1} and 5 wt% Cat.

of oxirane formation for different catalyst particle diameters (Fig. 5b). The progress of the oxirane concentration as a function of the reaction time was very similar for the different catalyst particle sizes. Because very fine particles (63–125 µm) were the dominating fraction, the operation within the regime of intrinsic kinetics was confirmed and no internal diffusion limitations whatsoever were expected.

In conclusion, no mass transfer limitations of any type were evidenced in the experiments. Therefore, these phenomena were excluded from the kinetic modelling.

4. Kinetic modelling

4.1. From reaction mechanisms to rate equations

Different reaction mechanisms have been proposed for the direct epoxidation of double bonds on solid alumina catalysts. Bonon et al. (Bonon et al., 2014) have summarized from a recent DFT study of the olefin epoxidation (Kuznetsov et al., 2011) possible reactions paths for the catalytic epoxidation on alumina. The mechanisms are displayed in Fig. 7. From the viewpoint of fundamental chemical thinking, the rival mechanisms are quite different, but they have a common feature: the formation of a hydroperoxyl adduct on the alumina surface. Thus, a common step for the reaction sequence is presumed to be the activation of OH ligands on the alumina surface through reaction with hydrogen peroxide (Rinaldi and Schuchardt, 2004), leading to the formation of a hydroperoxyl group and release of water from the catalyst surface. The hydroperoxyl group is then able to further react with unsaturated fatty acid ester. After several intermediate steps, the epoxide group is finally formed, and the epoxidized product is desorbed from the catalyst surface. Considerable amounts of water remain on the surface. In this sense, the Sharpless route (Fig. 7) and the stepwise mechanism proposed in the literature are similar (Suarez et al., 2009).

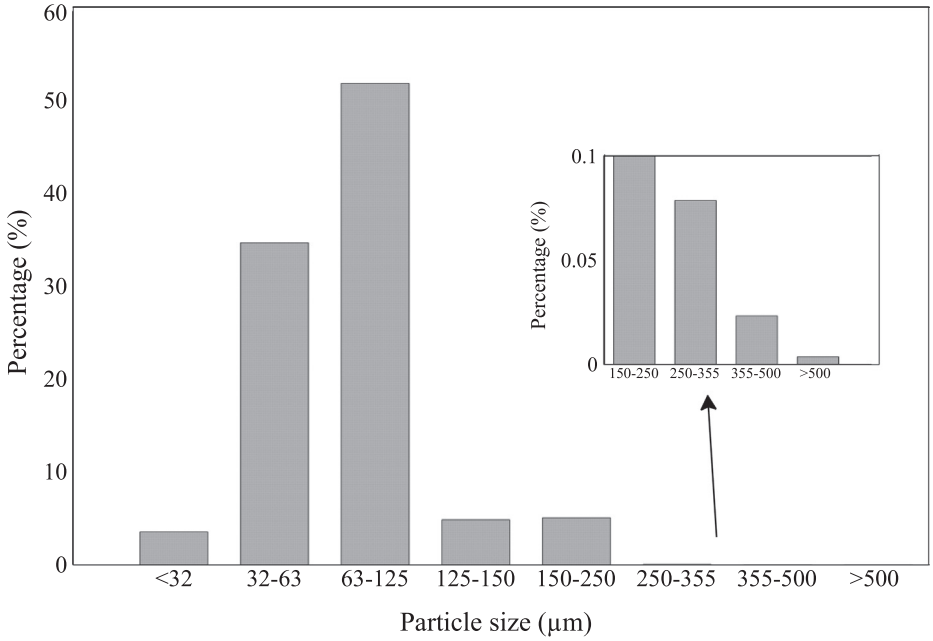

Fig. 6. Particle Size distribution of the catalyst.

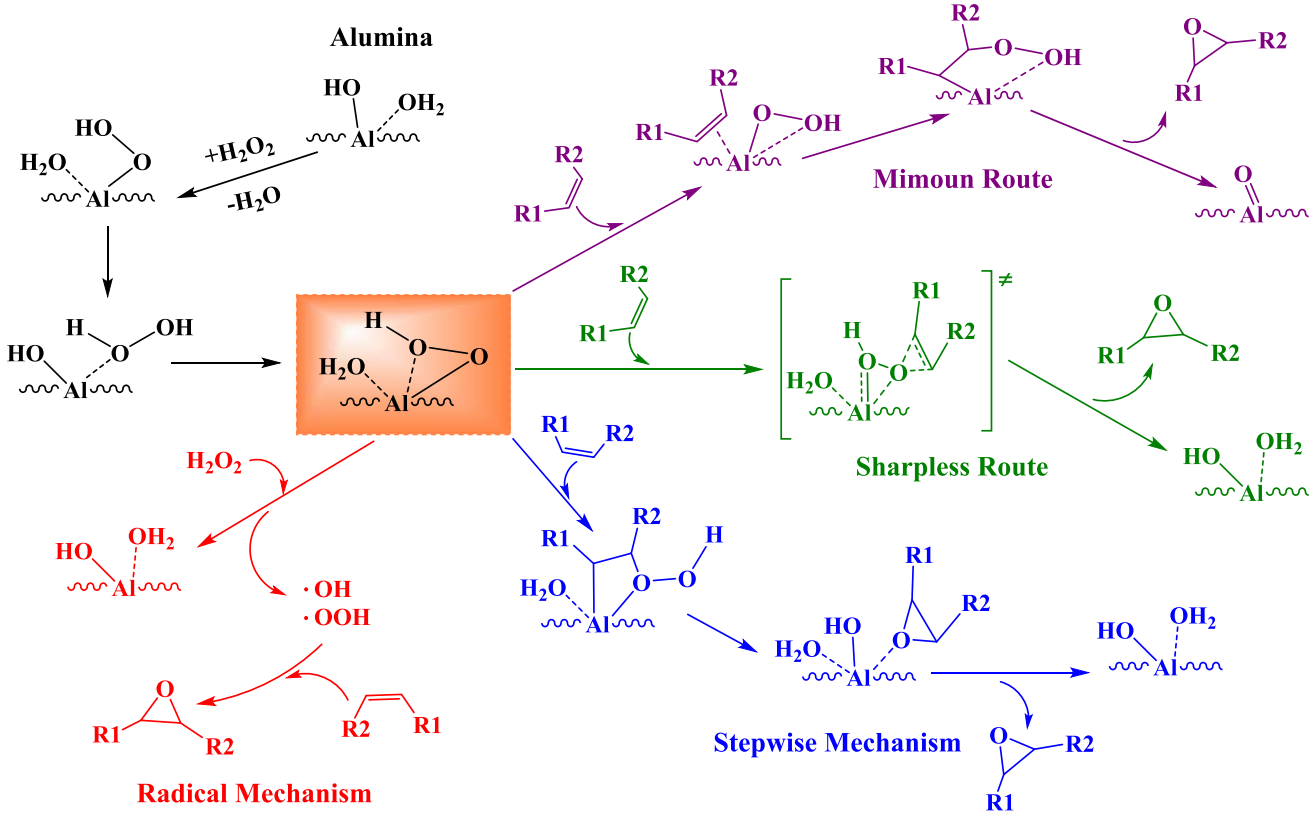

Fig. 7. Reaction mechanisms for the olefin epoxidation in the presence of an alumina catalyst.

A simple model is applied to the decomposition of hydrogen peroxide,

$$H_2O_2 \rightarrow H_2O + 1/2O_2$$

It is assumed that formed hydroperoxyl adduct (OOH*) releases oxygen into the liquid bulk phase, whereas adsorbed water (W*) remains on the catalyst surface until it is released from the surface via desorption or converted to OH. The decomposition mechanism of hydrogen peroxide can be written as

$$H_2O_2 + OH^* \rightarrow OOH^* + H_2O$$

$$OOH^* \rightarrow 1/2O_2 + OH^*$$

It should be noticed that the above equations are a simplification of the real surface reaction mechanism, probably proceeding stepwise, e.g.

$$H_2O_2 + * \rightarrow H_2O_2{}^*$$

$$H_2O_2{}^* + OH^* \rightarrow OOH^* + H_2O^*$$

$$H_2O^* \rightarrow H_2O + *$$

$$2OOH^* \rightarrow 2OH^* + O_2$$

4.2. Derivation of rate equations

4.2.1. Catalytic reactions

For the sake of brevity, the following abbreviations are used: hydrogen peroxide (HP), water (W), double bond (DB) and epoxide (EP) and surface intermediate (I). A summary of the simplified reaction mechanism can be provided as follows,

	ν_1	ν_2
1. HP + OH* = OOH* + W	1	1
2. OOH* → OH* + O	0	1
3. OOH* + DB → I*	1	0
4. I* → EP + OH*	1	0

Where the stoichiometric numbers ν_1 and ν_2 reflect the steps participating in the epoxidation and hydrogen peroxide decomposition routes. The sum of steps 1, 3 and 4 gives

DB + HP → EP + W double bond epoxidation Route I

While the sum of steps 1 and 2 gives

HP → W + O hydrogen peroxide decomposition Route II

where O denotes ½ O_2.

The first step is presumed to be reversible, whereas the other steps are taken as irreversible. The rate equations of the elementary steps are formulated in a standard manner,

$$r_1 = a_1 c_{OH*} - a_{-1} c_{OOH*} \quad (1)$$

$$r_2 = a_2 c_{OOH*} \quad (2)$$

$$r_3 = a_3 c_{OOH*} \quad (3)$$

$$r_4 = a_4 c_{I*} \quad (4)$$

where

$$a_1 = k_1 c_{HP} \quad (5)$$

$$a_{-1} = k_{-1} c_W \quad (6)$$

$$a_2 = k_2 \quad (7)$$

$$a_3 = k_3 c_{DB} \quad (8)$$

$$a_4 = k_4 \quad (9)$$

If quasi-steady state is assumed for all the adsorbed species, the stoichiometry gives the generation rates,

$$r_{OOH*} = r_1 - r_2 - r_3 = 0 \quad (10)$$

$$r_{OH*} = -r_1 + r_2 + r_4 = 0 \quad (11)$$

$$r_{I*} = r_3 - r_4 = 0 \quad (12)$$

Which confirms that $\Sigma r_{j^*} = 0$ and the total balance of available surface sites is expressed as

$$c_{OOH*} + c_{OH*} + c_{I*} = c_0 \quad (13)$$

where c_0 denotes the total concentration of the surface sites. Eqs. (10)–(13) contain three unknown concentrations (c_{OOH^*}, c_{OH^*}, and c_{I^*}). It should be noticed that the system (10)–(12) consists of two independent linear equations only: the sum of Eqs. (10) and (11) gives de facto Eq. (12). The concentration of OH ligands (c_{OH^*}) is solved from Eq. (10),

$$c_{OH*} = (a_{-1} + a_2 + a_3) c_{OOH*} / a_1 \quad (14)$$

And the concentration of the adsorbed intermediate (c_{I^*}) is solved from Eq. (12),

$$c_{I*} = a_3 c_{OOH*} / a_4 \quad (15)$$

The relations are inserted in the total balance (13), from which c_{OOH^*} is solved,

$$c_{OOH*} = a_1 a_4 c_0 (a_1 a_4 + (a_{-1} + a_2 + a_3) a_4 + a_1 a_3)^{-1} \quad (16)$$

The rate of the epoxide (EP) formation via the first route (I) is

$$r_4 = r_I = a_4 c_{I*} = a_3 c_{OOH*} \quad (17)$$

Which becomes

$$r_4 = r_I = \frac{a_1 a_3 a_4 c_0}{a_1 a_3 + a_1 a_4 + (a_{-1} + a_2 + a_3) a_4} \quad (18)$$

In an analogous manner, the rate of oxygen (O) formation via the second route is expressed as

$$r_2 = r_{II} = a_2 c_{OOH*} \quad (19)$$

The expression for c_{OOH^*} is inserted and we obtain

$$r_2 = r_{II} = \frac{a_1 a_2 a_4 c_0}{a_1 a_3 + a_1 a_4 + (a_{-1} + a_2 + a_3) a_4} \quad (20)$$

Finally, after division by $k_2 k_4$ and rearrangement the very compressed rate equations for the epoxidation and hydrogen peroxide decomposition are obtained,

$$r_I = \frac{k_I c_{DB} c_{HP}}{1 + \alpha c_{DB} + \beta c_{HP} + \gamma c_{DB} c_{HP} + \omega c_W} \quad (21)$$

$$r_{II} = \frac{k_{II} c_{HP}}{1 + \alpha c_{DB} + \beta c_{HP} + \gamma c_{DB} c_{HP} + \omega c_W} \quad (22)$$

where $k_I = (k_1 k_3 / k_2) c_0$, $k_{II} = k_1 c_0$, $\alpha = k_3/k_2$, $\beta = k_1/k_2$, $\gamma = k_1 k_3/(k_2 k_4)$ and $\omega = k_{-1}/k_2$. Rates r_I and r_{II} are the catalytic epoxidation and hydrogen peroxide decomposition rates, respectively. The operative parameters to be estimated by nonlinear regression analysis by using experimental data are k_I, k_{II}, β, γ and ω and their respective activation energies. Parameter α can be estimated through $k_I/k_{II} = \alpha$.

Some special cases are worth consideration. If adsorption of water is very rapid, k_{-1} is large and ω is large. Furthermore, if

the reaction of the double bond with the surface hydroperoxyl group, step 3 is slow, k_3 is small and consequently α and γ are small. During the parameter estimation process, various simplified forms of the rate equations were compared.

4.2.2. Non-catalytic reactions

For the non-catalytic reactions (r'_i) simple kinetic expressions were applied.

The empirical power-law expression was used for the hydrogen peroxide decomposition,

$$r'_{II} = k'_{II} \cdot c_{HP}{}^{\lambda} \tag{23}$$

The value of the exponent (λ) was adjusted in order to get the best possible fit to the experimental data.

It was also observed that non-catalytic epoxidation takes place in the system. Hence, some independent experiments without catalyst were carried out in order to have an acceptable approximation of this reaction rate. The kinetics of this process was described as follows,

$$r'_I = k'_I c_{HP} c_{DB} \tag{24}$$

Under the operating conditions used in this study, the influence of ring-opening reaction was observed to be low. The kinetics of ring-opening was described with the formula

$$r'_{RO} = k'_{RO} c_P \tag{25}$$

4.3. Component generation rates

The generation rates of the components are obtained as linear combinations of the rates r_{I} and r_{II}. The catalytic contributions to the generation rates are r_{I} and r_{II}, but the contributions of the non-catalytic reactions (r'_i) affect the generation rates, too.

The generation rates originating from heterogeneous catalysis are

$$r_{DB} = -r_I \tag{26}$$

$$r_{HP} = -r_I - r_{II} \tag{27}$$

$$r_{EP} = r_I \tag{28}$$

$$r_{O_2} = 0.5 r_{II} \tag{29}$$

$$r_W = r_I + r_{II} \tag{30}$$

And the generation rates related to the non-catalytic reactions, namely epoxidation, hydrogen peroxide decomposition and ring opening are

$$r'_{DB} = -r'_I \tag{31}$$

$$r'_{HP} = -r'_I - r'_{II} \tag{32}$$

$$r'_{EP} = r'_I - r'_{RO} \tag{33}$$

$$r'_{O_2} = 0.5 r'_{II} \tag{34}$$

$$r'_W = r'_I + r'_{II} \tag{35}$$

The generation rates are linked together in the semibatch reactor model.

5. Semibatch reactor model

5.1. General hypotheses for the reactor system

The kinetic experiments were conducted in the isothermal and isobaric reactor vessel. The sketch of the reactor system is shown in Fig. 1. Some experiments were carried out in complete batch mode, while the major part of the experiments were conducted in semibatch mode, in which the hydrogen peroxide solution was added gradually to the reaction mixture consisting of the esterified oleic acid, the heterogeneous catalyst and the solvent. Complete backmixing was assured for the reactor content because vigorous stirring (800 rpm) was applied, and the reactor was equipped with baffles; the external mass transfer resistance at the outer surface of the catalyst could thus be regarded negligible as discussed previously. The catalyst particle size was small (63–125 μm), which guaranteed the operation beyond the internal mass transfer limitations (pore diffusion) as treated previously. The perfectly mixed semibatch reactor model was considered sufficient for the quantitative interpretation of the experimental data on the epoxidation kinetics. Since the mass transfer phenomena was proved negligible, and for the sake of simplicity, one homogeneous phase was assumed for the mass balance.

5.2. Details of the semibatch reactor model

The volumes were assumed additive, which implies that a simple update formula for the liquid volume (V_{L}) is applied,

$$V_L = V_{0L} + V' t \tag{36}$$

where $V_{0\mathrm{L}}$ is the initial volume and V' is the volumetric flow rate (the feed rate of aqueous hydrogen peroxide solution). The mass balance equation for an arbitrary component can be written as

$$n'_{0i} + r_i m_{cat} + r'_i V_L = \frac{dn_i}{dt} \tag{37}$$

where $n'_{0\mathrm{i}}$ is the molar flow rate in the feed ($n'_{0\mathrm{i}} \neq 0$ for hydrogen peroxide (HP) and water (W), but $n'_{0\mathrm{i}} = 0$ for the other components), n_{i} is the amount of substance in the reactor and m_{cat} is the mass of catalyst. The terms r_{i} and r'_{i} denote the catalytic and non-catalytic generation rates of the components, respectively.

The inlet molar flow is expressed with the concentration in the feed ($c_{0\mathrm{i}}$) and the volumetric flow rate. The catalyst bulk density (ρ_{B}) is introduced: $\rho_{\mathrm{B}} = m_{\mathrm{cat}}/V_{\mathrm{L}}$. After inserting the update of the liquid volume, the expression for ρ_{B} becomes

$$\rho_B = \frac{\rho_{0B}}{1 + t/\tau_0} \tag{38}$$

where $\rho_{0\mathrm{B}} = m_{\mathrm{cat}}/V_{0\mathrm{L}}$ and $\tau_0 = V_{0\mathrm{L}}/V'$.

After inserting this relation to the mass balance Eq. (37), it becomes

$$\frac{dn_i}{dt} = c_{0i} V' + (r_i \rho_{0B} + r'_i (1 + t/\tau_0)) V_{0L} \tag{39}$$

The amount of substance (n_{i}) can be elaborated further, because $n_{\mathrm{i}} = c_{\mathrm{i}} V_{\mathrm{L}}$.

Differentiation gives

$$\frac{dn_i}{dt} = \frac{d(c_i V_L)}{dt} = \frac{dc_i}{dt} V_L + c_i \frac{dV_L}{dt} \tag{40}$$

According to Eq. (36), $\mathrm{d}V_{\mathrm{L}}/\mathrm{d}t = V'$. After inserting these relations into the balance equation, the mass balance becomes

$$\frac{dc_i}{dt} = \frac{(c_{0i} - c_i) V'}{V_L} + (r_i \rho_{0B} + r'_i (1 + t/\tau_0)) \frac{V_{0L}}{V_L} \tag{41}$$

where $V_{\mathrm{L}}/V_{0\mathrm{L}} = 1 + t/\tau_0$ and $V_{\mathrm{L}}/V' = t + \tau_0$

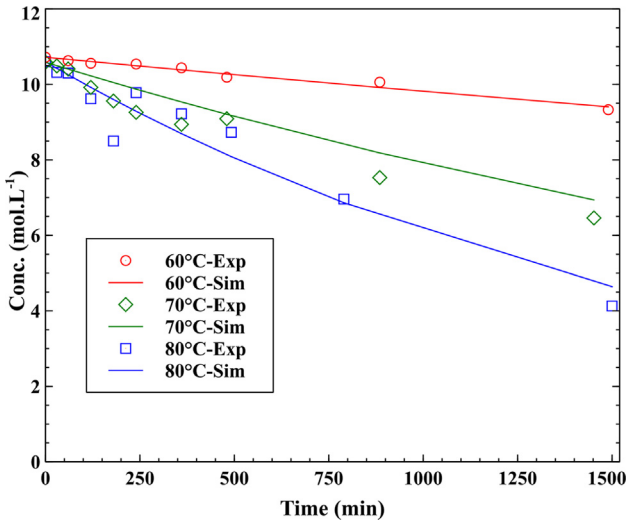

Fig. 8. Non-catalytic hydrogen peroxide decomposition: experimental results and model fit.

Table 3
Parameter estimation for the non-catalytic H_2O_2 decomposition at 70 °C.

	Estimated parameters	Estimated Std Error	Est. Relative Std Error (%)
k'_{II}	0.226E-03	0.290E-04	12.8
Ea'_{II}	0.897E + 05	0.129E + 05	14.4

Units: k'_{II} = (min^{-1}); Ea'_{II} = ($J{\cdot}mol^{-1}$).

The final form of the balance can be written as

$$\frac{dc_i}{dt} = \frac{(c_{0i} - c_i)/\tau_0}{1 + t/\tau_0} + \frac{r_i \rho_{0B}}{1 + t/\tau_0} + r'_i \tag{42}$$

Eq. (42) describes the changes of the concentrations of both batch and semibatch components. For batch components (DB and EP), the concentrations in the feed (c_{0DB}, c_{0EP}) are zero.

Table 4
Parameter estimation for the non-catalytic epoxidation.

	Estimated parameter	Estimated Std Error	Est. Relative Std Error (%)
k'_I	0.250E-03	0.464E-04	18.5
k'_{RO}	0.619E-03	0.246E-03	37.6
Ea'_I	0.100E + 06	0.376E + 05	39.8
Ea'_{RO}	0.128E + 06	0.117E + 06	91.6

Units: k'_I = ($L{\cdot}mol^{-1}{\cdot}min^{-1}$); k'_{RO} = (min^{-1}); Ea'_i = ($J{\cdot}mol^{-1}$).

5.3. Summary of the model and numerical aspects

The computational procedure is summarized as follows:

The rates of catalytic reactions were calculated from Eqs. (21) and (22). The rate of non-catalytic decomposition of hydrogen peroxide was calculated from Eq. (23), the rate of non-catalytic epoxidation from Eq. (24) and the rate of ring-opening from Eq. (25). The component generation rates were obtained from Eqs. (26)–(35). The generation rates were inserted in the differential Eq. (42), which were solved numerically with respect to the reaction time. The initial concentrations of the components in the reactor were all known, and they were used as the initial conditions for the differential Eq. (42).

The mass balance of oxygen was discarded in the calculations, because it did not have an effect on the other balances and the oxygen released to the gas phase was not measured. Arrhenius equation was assumed valid for the description of the temperature dependences of the rate constants. The correlations between the pre-exponential factors and the activation energies were suppressed by using a modified form of the Arrhenius equation. The computations were repeated several times with different sets of rate parameters in order to obtain the best fit of the model to the experimental data.

The differential Eq. (42) were solved with a stiff ODE solver algorithm (ODESSA) and the minimum of the error squares between experimentally recorded and predicted (Eq. (43)) concentrations was searched with a combined simplex-Levenberg-

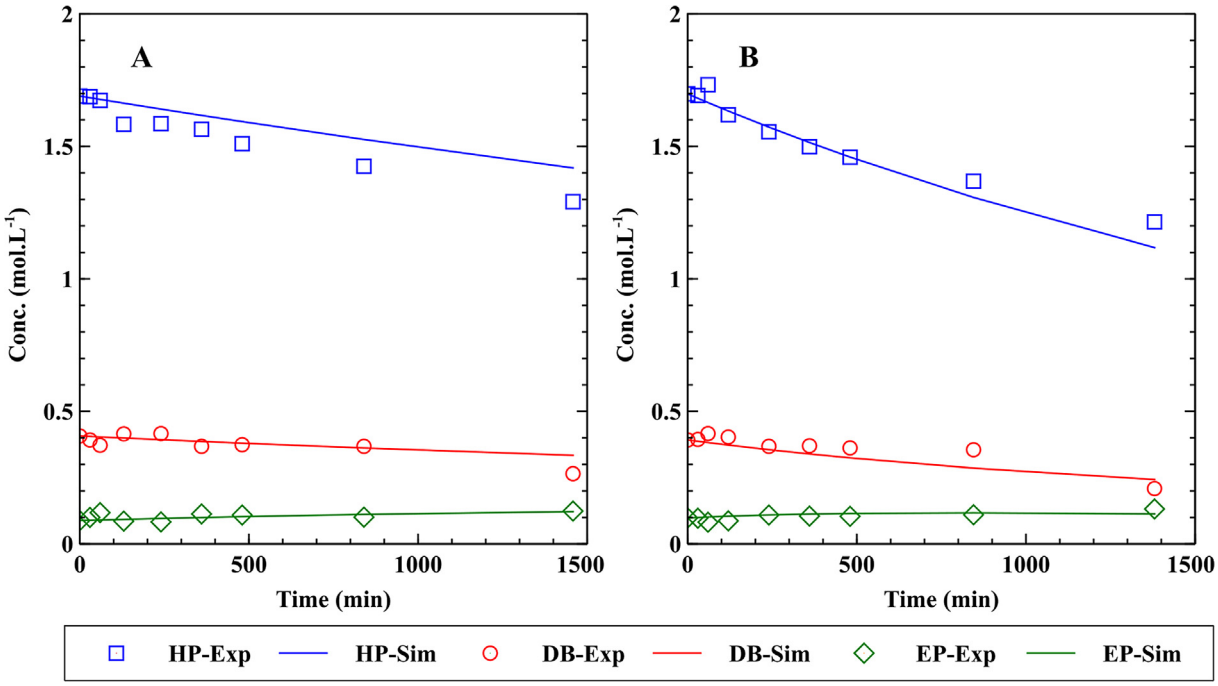

Fig. 9. Non-catalytic epoxidation at DB:HP = 1:4: experimental data and model fit; (A) 70 °C (B) 80 °C.

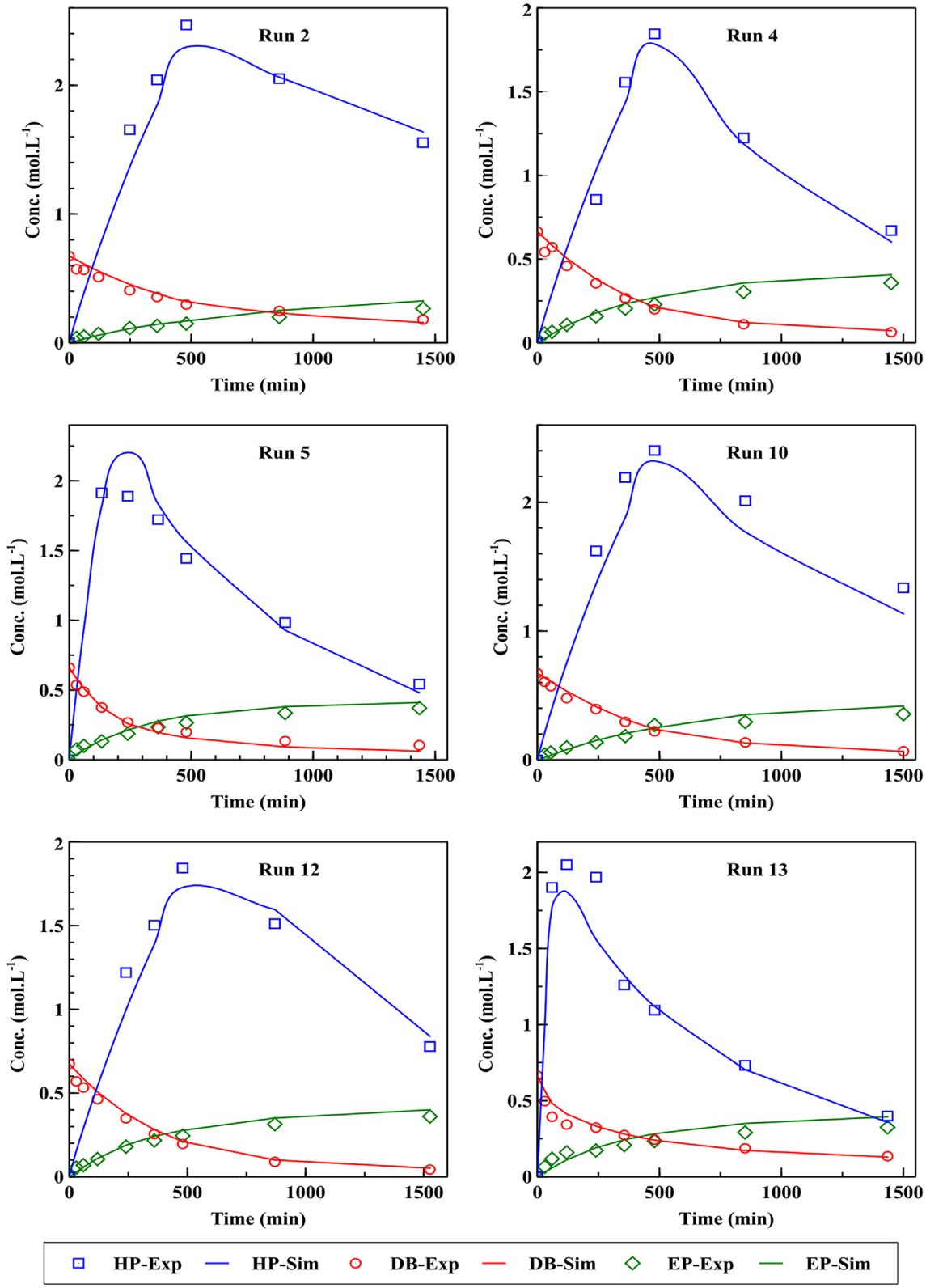

Fig. 10. Fit of the model to the experimental data for the alumina-catalyzed epoxidation of methyl oleate (Run number, see Table 2).

Marquardt algorithm. The software ModEst (Haario, 2011) was used to carry out the numerical operations. The objective function was defined as follows,

$$OF = \sum (C_{i,\mathrm{exp}} - C_{i,sim})^2 \tag{43}$$

The reliability of the model to adjust to the experimental data was evaluated by the coefficient of determination,

$$R^2 = 1 - \frac{\sum (C_{i,\mathrm{exp}} - C_{i,sim})^2}{\sum (C_{i,\mathrm{exp}} - \bar{C}_{i,\mathrm{exp}})^2} \tag{44}$$

6. Modelling results and discussion

6.1. Non-catalytic decomposition of hydrogen peroxide

The non-catalytic decomposition of hydrogen peroxide was studied separately from the heterogeneously catalyzed experiments. The decomposition experiments were conducted in batch mode, and the temperature was varied from 60 °C to 80 °C. A simple and adjustable power law expression as expressed by Eq. (23) was utilized and the reaction order was found to be around 1. Fig. 8 shows the fit of the model: the fit was very good and the R^2 coefficient exceeded 94%. The estimated values of the kinetic parameters are summarized in Table 3. The activation energy of the hydrogen peroxide decomposition was determined to be around 90 kJ/mol.

6.2. Non-catalytic epoxidation of methyl oleate

In addition to the non-catalytic hydrogen peroxide decomposition, it was evidenced that non-catalytic epoxidation took place in the system. In these experiments, a mixture of methyl oleate, hydrogen peroxide and ethyl acetate as the solvent was set to react in batch mode at different temperatures. The non-catalytic epoxidation was described with a simple model, Eq. (24) assuming elementary reaction steps and applying the steady-state approximation.

For the modelling of this homogenous reaction, previously obtained data of hydrogen peroxide decomposition was utilized. In addition, the simple expression Eq. (25) for the ring-opening was implemented. The ODE system formed from Eqs. (23)–(25) was solved numerically as a batch model.

The model fit is shown in Fig. 9. The model described the experimental data with a determination coefficient (Eq. (44)) exceeding 99.5%. It can be noticed from the figure that the non-catalytic epoxidation reaction proceeded at a slow rate, double bond and oxirane concentration change very little over time. On the other hand, the hydrogen peroxide concentration decreased rapidly due to the secondary non-catalytic decomposition.

The estimation results for the non-catalytic epoxidation are collected in Table 4. A good fit was accomplished with a considerably high error for the estimation of the ring-opening reactions, nevertheless still acceptable. The errors of the ring-opening parameters are reasonable, taking into account the complexity of this secondary reaction system, which has been studied previously by some researchers (Cai et al., 2018; Campanella and Baltanás, 2005; Tesser et al., 2020). These investigations have confirmed that ring-opening leads to a very wide range of products, and the product distribution is dependent on many parameters, conditions and intrinsic characteristics of the system. In this particular case, the estimated parameters for the ring-opening were not used further, but the ring-opening parameters were re-estimated for the catalytic epoxidation case.

6.3. Catalytic epoxidation of methyl oleate

After modelling the kinetics of the non-catalytic reactions, the modelling of the catalytic epoxidation process was proceeded. The non-catalytic kinetics was incorporated into the model, in the case of hydrogen peroxide decomposition a correcting factor V_{aq}/V_L was implemented, where V_{aq} is the aqueous phase volume and V_L de total reactor volume.

During the course of the parameter estimation, it was noticed that incorporating ring opening reactions did not give any essential improvement to the model. Unlike the previous non-catalytic epoxidation, the contribution of ring opening to the overall rates in this system was found to be negligible. Therefore, the impact of these reactions was neglected and excluded from the catalytic model. Also, the merged parameters β and γ were noticed to be of very low values compared to the rest of adsorption parameters. Thus, simplified versions of the rate expressions, Eqs. (21) and (22) were used, only taking into account k_I, k_{II}, ω and the α parameter (k_I/k_{II}), which were of importance in practice. In this sense, the total number of parameters estimated by regression analysis was reduced to six.

A quite good fit (>90%) was achieved. As illustrated in Fig. 10 the model describes in a well manner the experimental data, which is also confirmed by the parity plot (Fig. 11). The standard deviations of the parameters are of medium values (Table 5). Except in the case of parameter ω that was relatively high, possibly because of the water concentration being simulated. A moderate correlation between the kinetic constants at the reference temperature and the activation energies was observed as shown in the correlation matrix (Table 6).

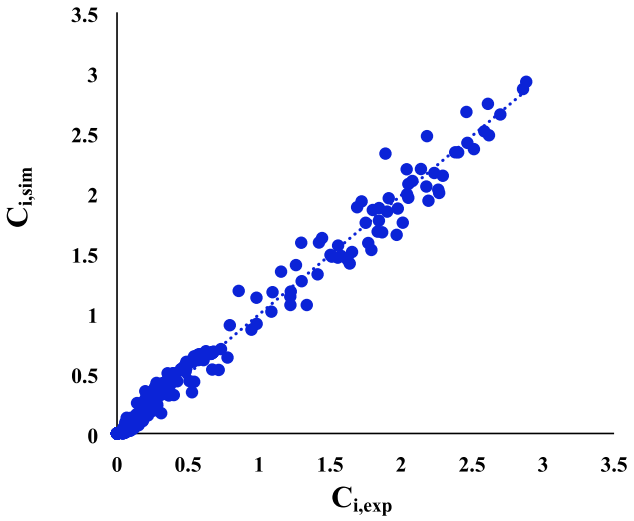

Fig. 11. Parity plot for the alumina-catalyzed epoxidation of methyl oleate as a model compound.

Table 5
Parameter estimation results for catalytic of methyl oleate epoxidation.

	Estimated parameter	Estimated Std Error	Est. Relative Std Error (%)
k_I	4.97E-05	1.87E-05	37.6
k_{II}	6.53E-05	2.38E-05	36.4
ω	2.00E-01	1.26E-01	63.2
Ea_I	1.01E + 05	3.56E + 04	35.3
Ea_{II}	1.22E + 05	2.14E + 04	17.5
Ea_ω	1.06E + 05	4.67E + 04	44

Units: k_I = ($L^2 \cdot mol^{-1} \cdot g^{-1} \cdot min^{-1}$); k_{II} = ($L \cdot g^{-1} \cdot min^{-1}$); ω = ($L \cdot mol^{-1}$); E_a = ($J \cdot mol^{-1}$).

Table 6
Correlation matrix of the kinetic parameters.

	k_I	k_{II}	ω	Ea_I	Ea_{II}	Ea_ω
k_I	1.000					
k_{II}	0.825	1.000				
ω	0.823	0.970	1.000			
Ea_I	0.024	0.299	0.222	1.000		
Ea_{II}	0.483	0.490	0.378	0.351	1.000	
Ea_ω	−0.15	−0.203	−0.391	0.264	0.615	1.000

7. Conclusions

It was found that the epoxidation of methyl oleate was significantly enhanced when applying a semibatch mode of operation. Dosing the hydrogen peroxide over an extended period of time enabled to maintain a good availability of this reactant in the system. Because the decomposition of hydrogen peroxide takes place rather rapidly, therefore, controlling this process was very essential for a more efficient epoxidation. During the experiments, it was observed that the concentration of hydrogen peroxide in the reactor was always higher in the semibatch operation mode when compared to the batch operation mode. Low flow rates of hydrogen peroxide improved the oxirane yield in more than a 30%.

A kinetic model was developed based on chemically plausible surface reaction mechanisms. The number of adjustable kinetic parameters to be estimated by regression analysis were reduced by studying independently the non-catalytic reactions in the system. The obtained model of the non-catalytic kinetics was integrated to the catalytic epoxidation kinetics. A good fit of the mathematical model was achieved by applying this strategy. The proposed kinetic model described very well the behavior of the system, and it can serve for further evaluations of similar heterogeneous system for the epoxidation of vegetable oils. With the modelling approach presented in this work, the optimal dosing policy and temperate for semibatch operation can be found.

CRediT authorship contribution statement

Wander Y. Perez-Sena: Methodology, Validation, Formal analysis, Investigation, Data curation, Writing - original draft, Writing - review & editing, Visualization. **Johan Wärnå:** Methodology, Formal analysis, Resources, Data curation. **Kari Eränen:** Validation, Investigation, Resources, Supervision. **Pasi Tolvanen:** Conceptualization, Methodology, Supervision. **Lionel Estel:** Conceptualization, Methodology, Resources, Supervision. **Sébastien Leveneur:** Conceptualization, Methodology, Supervision, Project administration, Funding acquisition. **Tapio Salmi:** Conceptualization, Methodology, Writing - original draft, Writing - review & editing, Supervision, Project administration, Funding acquisition.

Declaration of Competing Interest

The authors declare that they have no known competing financial interests or personal relationships that could have appeared to influence the work reported in this paper.

Acknowledgements

This work is part of the activities financed by Academy of Finland, the Academy Professor grants 319002 and 320115 (T. Salmi, P. Tolvanen). The economic support from Academy of Finland is gratefully acknowledged. The authors thank the Ministry of Higher Education, Science and Technology of Dominican Republic and the ERASMUS program for the support.

Appendix A. Supplementary material

Supplementary data to this article can be found online at https://doi.org/10.1016/j.ces.2020.116206.

References

Biermann, U., Bornscheuer, U., Meier, M.A.R., Metzger, J.O., Schäfer, H.J., 2011. Oils and Fats as Renewable Raw Materials in Chemistry. Angew. Chem. Int. Ed. 50 (17), 3854–3871. https://doi.org/10.1002/anie.201002767.

Bonon, A.J., Kozlov, Y.N., Bahú, J.O., Filho, R.M., Mandelli, D., Shul'pin, G.B., 2014. Limonene epoxidation with H 2 O 2 promoted by Al 2 O 3: Kinetic study, experimental design. J. Catal. 319, 71–86. https://doi.org/10.1016/j.jcat.2014.08.004.

Cai, X., Zheng, J.-L., Freites Aguilera, A., Vernères-Hassimi, L., Tolvanen, P., Salmi, T., Leveneur, S., 2018. Influence of ring-opening reactions on the kinetics of cottonseed oil epoxidation. Int. J. Chem. Kinet. 50 (10), 726–741. https://doi.org/10.1002/kin.21208.

Campanella, A., Baltanás, M.A., 2005. Degradation of the oxirane ring of epoxidized vegetable oils in liquid-liquid systems: Hydrolysis and attack by H2O2. Lat. Am. Appl. Res., 6

Campanella, A., Baltanás, M.A., Capel-Sánchez, M.C., Campos-Martín, J.M., Fierro, J.L.G., 2004. Soybean oil epoxidation with hydrogen peroxide using an amorphous Ti/SiO $_2$ catalyst. Green Chem 6 (7), 330–334. https://doi.org/10.1039/B404975F.

Cherubini, F., 2010. The biorefinery concept: Using biomass instead of oil for producing energy and chemicals. Energy Convers. Manag. 51 (7), 1412–1421. https://doi.org/10.1016/j.enconman.2010.01.015.

Danov, S.M., Kazantsev, O.A., Esipovich, A.L., Belousov, A.S., Rogozhin, A.E., Kanakov, E.A., 2017. Recent advances in the field of selective epoxidation of vegetable oils and their derivatives: a review and perspective. Catal. Sci. Technol. 7 (17), 3659–3675. https://doi.org/10.1039/C7CY00988G.

Eränen, K., 2004. Abatement of Nitric Oxide by Catalytic Decomposition and Selective Catalytic Reduction with Hydrocarbons. AAbo Akademi University.

Epoxidized Soybean Oil (ESBO) Market by Raw Material, Application, End-use Application & Geography | COVID-19 Impact Analysis | MarketsandMarkets. https://www.marketsandmarkets.com/Market-Reports/epoxidized-soybean-oil-market-27777113.html (accessed Jul. 06, 2020).

Freites Aguilera, A., Tolvanen, P., Heredia, S., Gonzales Munoz, M., Samson, T., Oger, A., Verove, A., Eränen, K., Leveneur, S., Mikkola, J.-P., Salmi, T., 2018. Epoxidation of Fatty Acids and Vegetable Oils Assisted by Microwaves Catalyzed by a Cation Exchange Resin. Ind. Eng. Chem. Res. 57 (11), 3876–3886. https://doi.org/10.1021/acs.iecr.7b05293.

Freites Aguilera, A., Tolvanen, P., Eränen, K., Wärnå, J., Leveneur, S., Marchant, T., Salmi, T., 2019. Kinetic modelling of Prileschajew epoxidation of oleic acid under conventional heating and microwave irradiation. Chem. Eng. Sci. 199, 426–438. https://doi.org/10.1016/j.ces.2019.01.035.

Goud, V.V., Patwardhan, A.V., Dinda, S., Pradhan, N.C., 2007. Kinetics of epoxidation of jatropha oil with peroxyacetic and peroxyformic acid catalysed by acidic ion exchange resin. Chem. Eng. Sci. 62 (15), 4065–4076. https://doi.org/10.1016/j.ces.2007.04.038.

Greenspan, F.P., MacKellar, D.G., 1948. Analysis of Aliphatic Per Acids. Anal. Chem. 20 (11), 1061–1063. https://doi.org/10.1021/ac60023a020.

Gunam Resul, M.F.M., López Fernández, A.M., Rehman, A., Harvey, A.P., 2018. Development of a selective, solvent-free epoxidation of limonene using hydrogen peroxide and a tungsten-based catalyst. React. Chem. Eng. 3 (5), 747–756. https://doi.org/10.1039/C8RE00094H.

Haario, H., 2011. MODEST User's guide. Profmath Oy Hels.

Horvath, I.T., Malacria, M., 2020. Advanced Green Chemistry - Part 2: From Catalysis To Chemistry Frontiers. World Scientific.

I. TC 34/SC 11, 2007. ISO 3961:1996, Animal and vegetable fats and oils – Determination of iodine value. Multiple. Distributed through American National Standards Institute.

Jay, R.R., 1964. Direct Titration of Epoxy Compounds and Aziridines. Anal. Chem. 36 (3), 667–668. https://doi.org/10.1021/ac60209a037.

Kuznetsov, M.L., Kozlov, Y.N., Mandelli, D., Pombeiro, A.J.L., Shul'pin, G.B., 2011. Mechanism of Al^{3+}-Catalyzed Oxidations of Hydrocarbons: Dramatic Activation of H2O2 toward O−O Homolysis in Complex $[Al(H_2O)^4(OOH)(H_2O_2]^{2+}$ Explains the Formation of HO• Radicals. Inorg. Chem. 50 (9), 3996–4005. https://doi.org/10.1021/ic102476x.

Lefèvre, G., Duc, M., Lepeut, P., Caplain, R., Fédoroff, M., 2002. Hydration of γ-Alumina in Water and Its Effects on Surface Reactivity. Langmuir 18 (20), 7530–7537. https://doi.org/10.1021/la025651i.

Li, J., Zhao, G., Gao, S., Lv, Y., Li, J., Xi, Z., 2006. Epoxidation of Allyl Chloride to Epichlorohydrin by a Reversible Supported Catalyst with H_2O_2 under Solvent-Free Conditions. Org. Process Res. Dev. 10 (5), 876–880. https://doi.org/10.1021/op060108k.

Mandelli, D., 2001. Alumina-catalyzed alkene epoxidation with hydrogen peroxide, pp. 5.

Miao, Y.X., Liu, J.P., 2014. Epoxidation of Soybean Oil under Acid-Free Condition. Adv. Mater. Res. 881–883, 140–143. https://doi.org/10.4028/www.scientific.net/AMR.881-883.140.

Mohanty, A.K., Misra, M., Drzal, L.T., 2002. Sustainable Bio-Composites from Renewable Resources: Opportunities and Challenges in the Green Materials World. J. Polym. Environ. 10 (1), 19–26. https://doi.org/10.1023/A:1021013921916.

Murawski, A., Quirino, R.L., 2018. Vegetable Oils as a Chemical Platform. In: Thakur, V.K., Thakur, M.K., Voicu, S.I. (Eds.), Polymer Gels: Perspectives and Applications. Springer, Singapore, pp. 125–152.

Nicolau, A., Mariath, R.M., Martini, E.A., dos Santos Martini, D., Samios, D., 2010. The polymerization products of epoxidized oleic acid and epoxidized methyl oleate with cis-1,2-cyclohexanedicarboxylic anhydride and triethylamine as the initiator: Chemical structures, thermal and electrical properties. Mater. Sci. Eng. C 30 (7), 951–962. https://doi.org/10.1016/j.msec.2010.04.014.

Nur, H., Ikeda, S., Ohtani, B., 2001. Phase-Boundary Catalysis of Alkene Epoxidation with Aqueous Hydrogen Peroxide Using Amphiphilic Zeolite Particles Loaded with Titanium Oxide. J. Catal. 204 (2), 402–408. https://doi.org/10.1006/jcat.2001.3386.

Osman, A.I., Abu-Dahrieh, J.K., Rooney, D.W., Thompson, J., Halawy, S.A., Mohamed, M.A., 2017. Surface hydrophobicity and acidity effect on alumina catalyst in catalytic methanol dehydration reaction. J. Chem. Technol. Biotechnol. 92 (12), 2952–2962. https://doi.org/10.1002/jctb.5371.

Paquot, C., 2013. Standard Methods for the Analysis of Oils, Fats and Derivatives. Elsevier.

Parada Hernandez, N.L., Bonon, A.J., Bahú, J.O., Barbosa, M.I.R., Wolf Maciel, M.R., Filho, R.M., 2017. Epoxy monomers obtained from castor oil using a toxicity-free catalytic system. J. Mol. Catal. Chem. 426, 550–556. https://doi.org/10.1016/j.molcata.2016.08.005.

Pérez-Sena, W.Y., Salmi, T., Estel, L., Leveneur, S., 2020. Thermal risk assessment for the epoxidation of linseed oil by classical Prisleschajew epoxidation and by direct epoxidation by H2O2 on alumina. J. Therm. Anal. Calorim. 140 (2), 673–684. https://doi.org/10.1007/s10973-019-08894-2.

Phimsen, S., Yamada, H., Tagawa, T., Kiatkittipong, W., Kiatkittipong, K., Laosiripojana, N., Assabumrungrat, S., 2017. Epoxidation of methyl oleate in a TiO_2 coated-wall capillary microreactor. Chem. Eng. J. 314, 594–599. https://doi.org/10.1016/j.cej.2016.12.017.

Richard, R., Thiebaud-Roux, S., Prat, L., 2013. Modelling the kinetics of transesterification reaction of sunflower oil with ethanol in microreactors. Chem. Eng. Sci. 87, 258–269. https://doi.org/10.1016/j.ces.2012.10.014.

Rinaldi, R., Schuchardt, U., 2004. Factors responsible for the activity of alumina surfaces in the catalytic epoxidation of cis-cyclooctene with aqueous H_2O_2. J. Catal. 227 (1), 109–116. https://doi.org/10.1016/j.jcat.2004.06.028.

Salem, I.A., Salem, M.A., Gemeay, A.H., 1993. Kinetics of heterogeneous decomposition of hydrogen peroxide with some transition metal complexes supported on silica-alumina in aqueous medium. J. Mol. Catal. 84 (1), 67–75. https://doi.org/10.1016/0304-5102(93)80085-9.

Santacesaria, E., Tesser, R., Di Serio, M., Turco, R., Russo, V., Verde, D., 2011. A biphasic model describing soybean oil epoxidation with H2O2 in a fed-batch reactor. Chem. Eng. J. 173 (1), 198–209. https://doi.org/10.1016/j.cej.2011.05.018.

Scotti, N., Ravasio, N., Psaro, R., Evangelista, C., Dworakowska, S., Bogdal, D., Zaccheria, F., 2015. Copper mediated epoxidation of high oleic natural oils with a cumene–O_2 system. Catal. Commun. 64, 80–85. https://doi.org/10.1016/j.catcom.2015.02.008.

Sengupta, A.K., 2017, Ion Exchange and Solvent Extraction: A Series of Advances, vol. 22. CRC Press.

Sepulveda, J., Teixeira, S., Schuchardt, U., 2007. Alumina-catalyzed epoxidation of unsaturated fatty esters with hydrogen peroxide. Appl. Catal. Gen. 318, 213–217. https://doi.org/10.1016/j.apcata.2006.11.004.

Sheldon, R.A., 2014. Green and sustainable manufacture of chemicals from biomass: state of the art. Green Chem. 16 (3), 950–963. https://doi.org/10.1039/C3GC41935E.

Stamatiou, I.K., Muller, F.L., 2017. Determination of mass transfer resistances of fast reactions in three-phase mechanically agitated slurry reactors. AIChE J. 63 (1), 273–282. https://doi.org/10.1002/aic.15540.

Suarez, P.A.Z., Pereira, M.S.C., Doll, K.M., Sharma, B.K., Erhan, S.Z., 2009. Epoxidation of Methyl Oleate Using Heterogeneous Catalyst. Ind. Eng. Chem. Res. 48 (7), 3268–3270. https://doi.org/10.1021/ie801635b.

Swern, Daniel, Findley, T.W., Billen, G.N., Scanlan, J.T., 1947. Determination of Oxirane Oxygen. Anal. Chem. 19 (6), 414–415. https://doi.org/10.1021/ac60006a018.

Tesser, R., Russo, V., Turco, R., Vitiello, R., Di Serio, M., 2020. Bio-lubricants synthesis from the epoxidized oil promoted by clays: Kinetic modelling. Chem. Eng. Sci. 214,. https://doi.org/10.1016/j.ces.2019.115445 115445.

Tuck, C.O., Pérez, E., Horváth, I.T., Sheldon, R.A., Poliakoff, M., 2012. Valorization of Biomass: Deriving More Value from Waste. Science 337 (6095), 695–699. https://doi.org/10.1126/science.1218930.

Turco, R., Pischetola, C., Tesser, R., Andini, S., Di Serio, M., 2016. New findings on soybean and methylester epoxidation with alumina as the catalyst. RSC Adv. 6 (38), 31647–31652. https://doi.org/10.1039/C6RA01780K.

Turco, R., Vitiello, R., Tesser, R., Vergara, A., Andini, S., Di Serio, M., 2017. Niobium Based Catalysts for Methyl Oleate Epoxidation Reaction. Top. Catal. 60 (15–16), 1054–1061. https://doi.org/10.1007/s11244-017-0808-y.

Vianello, C., Piccolo, D., Lorenzetti, A., Salzano, E., Maschio, G., 2018. Study of Soybean Oil Epoxidation: Effects of Sulfuric Acid and the Mixing Program. Ind. Eng. Chem. Res. 57 (34), 11517–11525. https://doi.org/10.1021/acs.iecr.8b01109.

Wu, X., Wang, M., Xie, Y., Chen, C., Li, K., Yuan, M., Zhao, X., Hou, Z., 2016. Carboxymethyl cellulose supported ionic liquid as a heterogeneous catalyst for the cycloaddition of CO_2 to cyclic carbonate. Appl. Catal. Gen. 519, 146–154. https://doi.org/10.1016/j.apcata.2016.04.002.

Zapata, R.B., Villa, A.L., de Correa, C.M., Ricardez-Sandoval, L., Elkamel, A., 2010. Dynamic Modeling and Optimization of a Batch Reactor for Limonene Epoxidation. Ind. Eng. Chem. Res. 49 (18), 8369–8378. https://doi.org/10.1021/ie100737y.

Zheng, J.L., Burel, F., Salmi, T., Taouk, B., Leveneur, S., 2015. Carbonation of Vegetable Oils: Influence of Mass Transfer on Reaction Kinetics. Ind. Eng. Chem. Res. 54 (43), 10935–10944. https://doi.org/10.1021/acs.iecr.5b02006.